Research Paper

IRA Journal of Engineering Science and Technology

Available online https://e-journals.irapublishing.com/index.php/IRAJEST

Vol.1, No.1, 2025, pp. 33-39, e-ISSN: XXXX- XXXX

https://doi.org/10.56862/irajest.v1i1.303

Testing of a Thermoelectric Generator (TEG) Using Heat from a Satay Furnace

Lolo Suhenra Simamora[1], Jufrizal[1*], Suherman[2], Asrul[3]

[1]Department of Mechanical Engineering, Universitas Medan Area, Medan 20223, Indonesia
[2]Department of Mechanical Engineering, Universitas Muhammadiyah Sumatera Utara, Medan 20238, Indonesia
[3]Software Engineering, SMK Negeri 5 Telkom Banda Aceh, Banda Aceh 23125, Indonesia
*Corresponding author: simamorasuhendra@gmail.com

Received: **2025-06-01** Revised: **2025-06-13** Accepted: **2025-06-28** Published: **2025-06-30**

Abstract

This study tested TEGs that utilize the heat of the satay furnace. The purpose of the research is to map heat transfer to the TEG module. The next goal is to measure the voltage, current, and electrical power generated. The test was conducted experimentally at six combustion time intervals. The parameters measured include hot side and cold side temperature, ΔT, voltage, and current. The estimated heat transfer was calculated using a simple radiation and conduction model. The results show a maximum power of 0.65 W at TEG-3 at 3,600 s. This condition is achieved at ΔT ≈ 46.7 °C with a voltage of 2.18 V and a current of 0.30 A. The lowest power of 0.53 W is recorded at TEG-2 at 3,600 s. The increase in ΔT is directly proportional to the rise in power in the test range. These results confirm the potential of satay kiln waste heat as a source of micropower.

Keywords: Heat transfer, Satay Furnace, Seebeck effect, Thermoelectric generator.

1. Introduction

Various sectors of life require reliable, affordable, and sustainable electrical energy [1-2]. The increase in population and economic activity places a greater burden on the electricity system [3-4]. Distribution networks face daily and seasonal variations in demand. Efforts to conserve energy are essential, but harvesting wasted heat is also crucial [5-7]. Thermoelectric technology enables the conversion of heat into electricity without the need for moving parts [8-9]. The working principle of this technology rests on the different temperatures of the material interface. The TEG module generates voltage when the hot side and the cold side have adequate ΔT [10-11].

Medium-temperature heat sources are suitable for small-scale TEG applications. Satay stoves provide a relatively stable heat profile during the combustion process. Culinary MSMEs use this furnace for repeated operational durations [12]. Wasted heat has the potential to become micropower for light loads. Micropower can supply lighting, sensors, and small battery charging [13]. The use of waste heat strengthens the concept of the energy circular economy [14-15]. This application also reduces emissions from thermal energy waste [16-17]. Technical challenges remain present in open burning environments.

A fluctuating flame converts the heat flux to the module [18-20]. The distance of the module to the heat source affects the ΔT in a real way. The performance of the cold-side heatsink determines the temperature stability. The quality of thermal insulation also controls heat loss to

the environment. Mechanical materials and joints must withstand thermal cycles. Soot and combustion residue can lower the thermal contact of the interface. This study assesses the feasibility of hot harvesting of satay kilns with TEG. The focus of the survey includes ΔT, voltage, current, and power mapping. The study also observed trends in radiant heat transfer and conduction.

Mathematically, conduction heat transfer is calculated as:

$$q = - kA\, dT/dx \quad (1)$$

And the heat transfer of radiation is calculated as:

$$q = \varepsilon.\sigma.A.(\Delta T^4) \quad (2)$$

Repeated measurements are taken at reasonable operating time intervals. The distance adjustment strategy is implemented to compensate for the temperature difference. This approach aims to strike a balance between performance and safety. The expected output is in the form of a map of TEG's performance in real scenarios. This map will guide the placement of the modules and the design of the cooling. The results of the research provide a design basis for the implementation of MSMEs. Its practical contribution is a simple, replicable test model. His scientific contribution is the association of ΔT with the electrical output at the load. This framework opens up DC–DC integration options and charge management. Technical recommendations aim to enhance the thermal stability of the system. Further research will evaluate the durability of the modules under various cycling conditions. A measured approach is expected to encourage the adoption of technology on a small scale.

2. Methods

The research used a controlled experimental approach. The scheme of the method is shown in Figure 1. Six TEG modules are arranged in series–parallel to obtain the working voltage. The output of the TEG is routed to the Battery Management System (BMS). The BMS regulates the protection and charging of the battery. The battery then supplies the lights as a verification load.

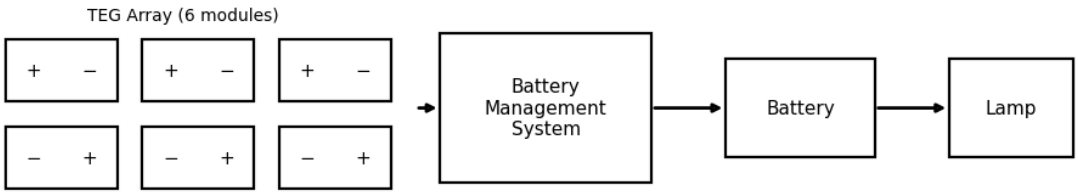

Figure 1. Diagram system

The heat source comes from a charcoal-fired satay stove. The TEG module is placed at a distance of 6 cm from the hot surface. The heatsink is mounted on the cold side to keep ΔT. The temperature of the hot side and the cold side is measured with a thermogun. Voltage and current are measured with a digital multimeter. Data recording was carried out at 600, 1200, 1800, 2400, 3000, and 3600 s.

3. Results and Discussion

Measurements are focused on two key locations. The first location is on the hot surface of the skewer furnace. The second location is on the surface of the Peltier plate (cold side). The goal is to map the temperature trend to the time of combustion. Summary results are presented in Tables 1 and 2.

Table 1 shows that the surface temperature of the furnace increases over time. The average temperature rose from 127.8 °C at 600 s to 197.0 °C at 3,600 s. The peak value of a single sensor (T1) was recorded at 224.7 °C at 1,800 s. This trend confirms the continuous heat supply during the combustion process. Slight variations between sensors (T1–T3) are still visible. This variation is natural in open flames and ambient airflow.

Table 1. Test results on the hot surface of the satay furnace

Waktu (s)	T1 (°C)	T2 (°C)	T3 (°C)	Average (°C)
600	196.10	108.20	79.10	127.80
1200	223.70	134.70	139.00	165.80
1800	224.70	175.80	165.20	188.57
2400	213.10	183.60	177.90	191.53
3000	216.10	181.10	180.40	192.70
3600	219.10	182.40	189.60	197.03

Table 2 records the temperature response on the peltier plate. The average cold side temperature rises from 35.93 °C at 600 s. The average highest value was reached at 1,800 s, corresponding to a temperature of 64.03 °C. After that, fluctuations occurred at 2,400–3,000 s. The average returns increase at 3,600 s = 62.23 °C. Fluctuations are affected by fire dynamics, thermal contact, and heat release to the environment. The performance of the heatsink also determines the stability of the cold side.

Table 2. Test results on the hot surface of the peltier plate

Waktu (s)	T1 (°C)	T2 (°C)	T3 (°C)	Average (°C)
600	35.20	37.20	35.40	35.93
1200	45.60	51.20	51.20	49.33
1800	69.20	57.20	65.20	64.03
2400	62.10	50.70	50.30	54.16
3000	59.80	49.40	58.70	55.50
3600	69.20	57.80	59.70	62.23

The average temperature difference between the hot surface and the peltier plate increases with time. The difference is about 91.9 °C at 600 s and reaches ±134.8 °C at 3,600 s. This gap is an indicator of the potential practical temperature difference (ΔT) in the TEG module. Larger gaps usually increase the output voltage and power. However, the stability of the ΔT is still affected by the variation of flame, contact conduction, and thermal resistance of the interface.

Overall, the temperature data support the system's basic assumptions. The heat source provides sufficient thermal energy for 1 hour of operation. The peltier side responds with a measured rise accompanied by reasonable fluctuations. These results form the basis for the discussion of TEG's electrical performance in the next section. The practical impact is the need for flame control and heatsink optimization. The goal is to keep the ΔT high and stable at real loads.

Figure 2 shows the hot surface temperature rising sharply to 1,800 s. The T1 sensor peaked at about 225 °C earlier. The T2 and T3 sensors follow with a more sloping slope. Variations between sensors remained noticeable throughout the test. This variation is natural in open flames and free air currents. After 1,800 s, the temperature tends to stabilize close to 190–200 °C. Figure 3 confirms this pattern through an average curve that climbs and then flattens. This stability indicates that the burning of charcoal has entered a steady phase. The coal layer becomes more homogeneous, and the heat flow is more consistent.

The cold side shows a different response. Figure 4 shows a rapid rise to 1,800 s. The value then dropped at 2,400–3,000 s and then recovered at 3,600 s. Figure 5 confirms the average fluctuation at 54–62 °C. Fluctuations occur due to three main factors. First, the thermal contact between the module and the heatsink is not yet constant. Secondly, the heat discharge into the air changes according to the blow and the geometry of the flame. Third, soot buildup interferes with local conduction. These results emphasize the importance of regulating the airflow around the heatsink. Emphasis is also necessary on the strength of the clamps and the material of the thermal interface.

The immediate consequence is seen in the difference in effective temperature. Figure 6 shows a clear distance between the hot and cold curves. Figure 7 shows ΔT increasing from ~92 °C to ~138 °C over 2,400 s. The value then decreased slightly but remained high at 3,600 s. The increase in ΔT is in line with the Seebeck effect. The voltage and power will increase as the ΔT increases. However, the local ΔT on the module can be smaller than the average difference. The cause is contact resistance and heat dispersion on the plate. This is why the best module peak power is recorded when the macro ΔT is not maximum. The module with the best contacts will give the highest output.

These visual findings provide clear technical direction. Keep a distance of 6 cm, but stabilize the flame pattern with a simple baffle. Increase cold side heat dissipation with wider fins. Forced ventilation or shallow water flow may be considered. Use thermal paste and constant torque clamps on the module interface. Clean soot periodically to lower contact resistance. Integrate DC–DC with MPPT to maximize the point of work. These measures target high and stable ΔT. The result is more consistent TEG power at real loads.

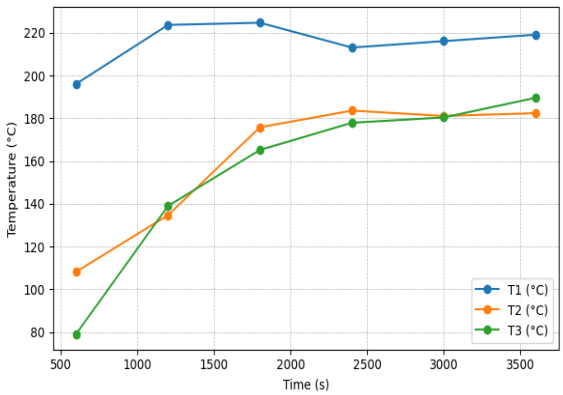

Figure 2. Hot surface temperature

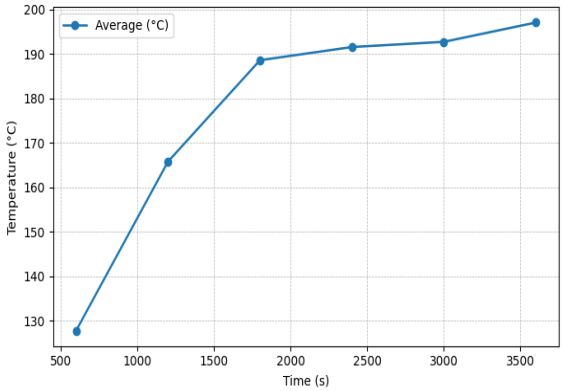

Figure 3. Hot surface average temperature

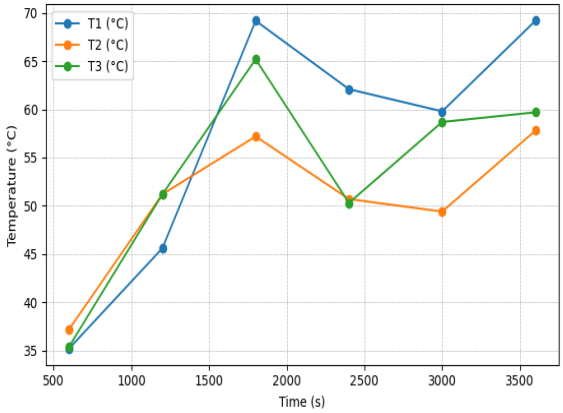

Figure 4. Cold-plate (Peltier) temperature

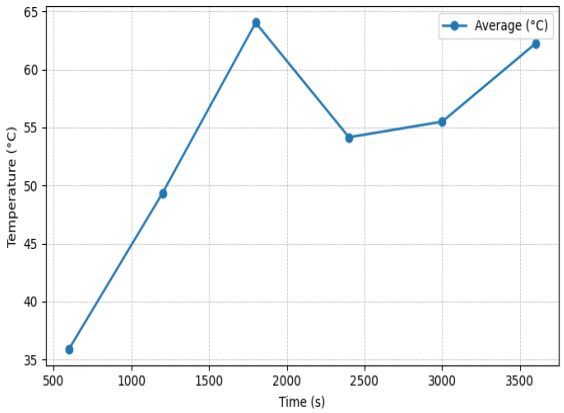

Figure 5. Cold-plate average temperature

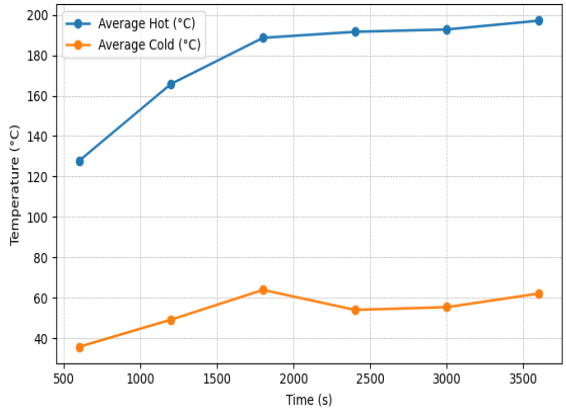

Figure 6. Average hot versus cold temperature

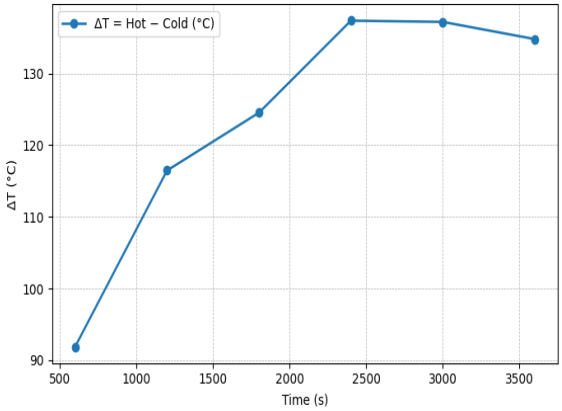

Figure 7. Effective ΔT versus time

4. Conclusion

This study demonstrates that the heat of the satay oven can be harnessed as a source of micropower. The temperature profile rises rapidly to a steady phase in the range of 190–200 °C. The cold side follows an uptrend with fluctuations due to contact and heat dissipation. The difference in effective temperature increases to a high range and then stabilizes. A distance of 6 cm from the heat source provides better heat flow. The best module reaches ΔT at about 46.7 °C at 3,600 s. The maximum power is recorded at 0.65 W on the TEG-3 at 3,600 s. The lowest power of 0.53 W occurs in TEG-2 at the same duration. Performance is greatly influenced by thermal contact quality and flame stability. The BMS–battery–lamp scheme works as a validation of real loads. The test results confirm the feasibility of the TEG for light lighting applications. The results also verify its potential for small battery charging.

Recommendations are designed to enhance heat stability, improve thermal interface quality, and optimize power conversion efficiency. Flames tend to be more stable when a simple baffle or a low-speed blower controls the airflow. The heat dissipation on the cold side needs to be strengthened to keep the ΔT high throughout operation. Wider heatsink fins or shallow water circulation consistently help lower thermal resistance. The module interface requires reliable contact management through thermal paste and clamps with constant torque. Soot residues and oxides should be cleaned periodically, as this layer increases the conduction resistance of the joints.

The geometry arrangement has a tangible impact on the heat flow and safety of the system. A distance of about six centimeters from the heat source shows good performance when equipped with a directed radiation shield. Power conversion becomes more effective with the addition of DC–DC boost and mini MPPT so that the module's working point is at the optimal voltage. Charging reliability and battery life are maintained through the BMS with adequate current, temperature, and voltage protection. Evaluation accuracy increases when the temperature is measured directly on both sides of the module, not just in the surrounding environment. Advanced validation can be done through replication with different fuel variations and load patterns. Long-term durability should be assessed through cyclic thermal fatigue tests on modules. Efficiency reporting from the heat inlet to the load power provides the basis for gradual improvements. At the same time, the modular mechanical design makes it easy to maintain and improve performance in the field.

Acknowledgments

The author expressed his gratitude to the Mechanical Engineering Laboratory of the University of Medan Area for the support of testing facilities and measurement instruments.

Appreciation was given to the Mechanical Engineering Study Program, which provided workshops and technician assistance during assembly and data acquisition. Thanks were also extended to colleagues for their methodological input and internal review, which improved test designs and manuscripts. The final award goes to the team of students who helped with temperature recording, data processing, and graphing, without mentioning one by one.

References

[1] T. Prasad, C. Nikhil, C. Sukrut, J. Suraj, and M. Piyush, "Solar-Powered Electric Vehicle Battery Charging: Integrating LT8490 for Sustainable and Efficient Energy Transfer in the Pursuit of a Green Transportation Future," in *2024 IEEE International Students' Conference on Electrical, Electronics and Computer Science (SCEECS)*, IEEE, Feb. 2024, pp. 1–6. doi: 10.1109/SCEECS61402.2024.10482005.

[2] M. Idris, A. F. Abdul Rasid, M. Mohd Zamberi, and Y. Zhang, "Biodiesel Production from Waste Cooking Oil: A Review of Prospects and Challenges," *Journal of Advanced Research in Fluid Mechanics and Thermal Sciences*, vol. 124, no. 1, pp. 28–52, Nov. 2024, doi: 10.37934/arfmts.124.1.2852.

[3] I. Wahyu Setya Andani, A. Sugiyono, K. Khotimah, and B. Desryanto Siregar, "Decarbonizing the electricity system in Sumatra region using nuclear and renewable energy based power generation," *IOP Conf Ser Earth Environ Sci*, vol. 753, no. 1, p. 012011, May 2021, doi: 10.1088/1755-1315/753/1/012011.

[4] C. Z. Yee *et al.*, "Developing a solar PV system for cost-effective electricity reduction in an aluminium extrusion plant," *IOP Conf Ser Earth Environ Sci*, vol. 1372, no. 1, p. 012081, Jul. 2024, doi: 10.1088/1755-1315/1372/1/012081.

[5] M. Idris *et al.*, "Engine Performance Using Blended Fuels of Biodiesel and Eco Diesel," *Energy Engineering*, vol. 120, no. 1, pp. 107–123, 2023, doi: 10.32604/ee.2023.019203.

[6] Randa Pratama, Muhammad Idris, Zakir Husin, Zainal Arif, Iskandar Yakoeb, and Supriadi, "Transesterification reaction time impacts on oxidation stability and acid number of biodiesel production from waste cooking oil," *JTTM : Jurnal Terapan Teknik Mesin*, vol. 5, no. 2, pp. 337–342, Oct. 2024, doi: 10.37373/jttm.v5i2.1220.

[7] M. Idris, M. Mohd Zamberi, A. Fuad Abdul Rasid, Y. Zhang, E. P. Salim Siregar, and U. Novalia Harahap, "Sustainable Biodiesel Production with Heterogeneous Catalysts: Insights from a Systematic Literature Review," *Journal of Advanced Research in Micro and Nano Engineering Journal homepage*, vol. 37, pp. 1–23, 2025, doi: 10.37934/armne.37.1.123.

[8] A. Kharina *et al.*, "The potential economic, heath, and greenhouse gas benefits of incorporating used cooking oil into Indonesia's biodiesel," 2018. [Online]. Available: www.theicct.orgcommunications@theicct.org

[9] Z. Pan, J. A. Weibel, and S. V. Garimella, "Transport mechanisms during water droplet evaporation on heated substrates of different wettability," *Int J Heat Mass Transf*, vol. 152, p. 119524, May 2020, doi: 10.1016/j.ijheatmasstransfer.2020.119524.

[10] D. Lee, K. Jeon, Y. Kim, and S. Jung, "Performance evaluation of coreless axial flux permanent magnet wind generator," in *2015 IEEE Magnetics Conference (INTERMAG)*, IEEE, May 2015, pp. 1–1. doi: 10.1109/INTMAG.2015.7156827.

[11] R. Wiranata and M. Idris, "Penyelidikan Eksperimental Alat Pengisi Daya Menggunakan Termoelektrik Dengan Pemanfaatan Panas Knalpot Sepeda Motor," *Jurnal Ilmiah Teknik Mesin & Industri (JITMI)*, vol. 2, no. 1, pp. 21–30, Jun. 2023, doi: 10.31289/jitmi.v2i1.1950.

[12] W. Li *et al.*, "Structural engineering of double shells decoration for preparing a high-efficiency electromagnetic wave absorber," *Ceram Int*, no. January, 2023, doi: 10.1016/j.ceramint.2023.01.044.

[13] S. Bhandari Abhi *et al.*, “An intelligent wind turbine with yaw mechanism using machine learning to reduce high-cost sensors quantity,” *Indonesian Journal of Electrical Engineering and Computer Science*, vol. 31, no. 1, p. 10, Jul. 2023, doi: 10.11591/ijeecs.v31.i1.pp10-21.
[14] R. N. Moulita, R. Rusdianasari, and L. Kalsum, “Biodiesel Production from Waste Cooking Oil using Induction Heating Technology,” *Indonesian Journal of Fundamental and Applied Chemistry*, vol. 5, no. 1, pp. 13–17, Feb. 2020, doi: 10.24845/ijfac.v5.i1.13.
[15] V. Ganapathy, *Steam generators and waste heat boilers: For process and plant engineers*. 2014. doi: 10.1201/b17519.
[16] S. K. Ramoji and L. C. Saikia, “Utilization of electric vehicles in combined voltage-frequency control of multi-area thermal-combined cycle gas turbine system using two degree of freedom tilt-integral-derivative controller,” *Energy Storage*, vol. 3, no. 4, Aug. 2021, doi: 10.1002/est2.234.
[17] R. Jayabal, G. M. Lionus Leo, M. Chrispin Das, S. Sekar, and S. Arivazhagan, “Impact of ammonia energy fraction on improving thermal efficiency and emissions of ammonia/biodiesel in dual fuel diesel engine,” *Process Safety and Environmental Protection*, vol. 188, pp. 1398–1410, Aug. 2024, doi: 10.1016/j.psep.2024.06.016.
[18] A. Fateev, “Flame, Combustion and Explosion Thermometry,” *Johnson Matthey Technology Review*, vol. 67, no. 1, pp. 25–35, Jan. 2023, doi: 10.1595/205651323X16643556587827.
[19] Y. Wang and S. H. Chung, “Soot formation in laminar counterflow flames,” *Prog Energy Combust Sci*, vol. 74, pp. 152–238, Sep. 2019, doi: 10.1016/j.pecs.2019.05.003.
[20] H. Yan *et al.*, “Thermodynamics Irreversibilities Analysis of Oxy-Fuel Diffusion Flames: The Effect of Oxygen Concentration,” *Entropy*, vol. 24, no. 2, p. 205, Jan. 2022, doi: 10.3390/e24020205.